

Orientation-Controlled Self-Assembled Nanolithography Using a Polystyrene–Polydimethylsiloxane Block Copolymer

Yeon Sik Jung and C. A. Ross*

Department of Materials Science and Engineering, Massachusetts Institute of Technology, Cambridge, Massachusetts 02139

Received April 19, 2007; Revised Manuscript Received May 25, 2007

ABSTRACT

Templated self-assembly of a cylinder-forming poly(styrene-*b*-dimethylsiloxane) (PS–PDMS) diblock copolymer has been investigated for nanolithography applications. The large χ -parameter of the blocks and the use of a PDMS–brush substrate surface treatment are especially advantageous for achieving long-range ordering and minimizing defect densities, and the high Si content in PDMS leaves a robust oxide etch mask after two-step reactive ion etching. By adjusting mesa width and solvent-annealing vapor pressure and time, the cylinders can be intentionally oriented parallel or perpendicular to the trench walls. Pattern transfer into thin silica is also demonstrated. This block copolymer system has excellent characteristics for self-assembled nanolithography applications.

The growing demand for nanoscale fabrication methods, combined with the inherent feature-size limitations of optical lithography and the low throughput of electron-beam lithography, have motivated a search for cost-effective nanoscale fabrication technologies, including nanoimprint lithography,¹ dip-pen nanolithography,² and block copolymer lithography.^{3–6} In the case of block copolymer lithography, the use of a chemical or topographical template enables control over the long-range order of the self-assembled patterns, providing a simple and scalable nanopatterning method in which the feature sizes and geometries are controlled via the chain length and volume fractions of the block copolymer.

In block copolymer lithography, arrays of holes or dots may be defined using a spherical-morphology block copolymer^{3,5,6} or a cylindrical-morphology block copolymer with the cylinders oriented perpendicular to the substrate.^{7,8} In contrast, patterns consisting of parallel lines may be defined using a cylindrical-morphology block copolymer with the cylinders parallel to the surface^{9–12} or a lamellar block copolymer with a perpendicular orientation.^{13,14} Such patterns have been templated using both chemical and topographical substrate features. For example, lamellar poly(styrene-*b*-polymethyl methacrylate) (PS–PMMA) patterns have been templated using a self-assembled monolayer patterned by extreme ultraviolet interference lithography (EUV-IL) or electron-beam (e-beam) lithography and have attracted much attention due to their high aspect ratio and absence of

defects.^{13,14} However, this process requires template generation on the same length scale as the period of the block copolymer.¹⁵ On the other hand, well-ordered arrays of in-plane cylinders templated by larger scale topographic patterns have been demonstrated by several groups. Horizontal cylinders from diblocks such as poly(styrene-*b*-ethylene propylene) (PS–PEP)⁹ and PS–PMMA^{10–12} have been successfully aligned in templates. The templates have critical dimensions an order of magnitude or more larger than the block copolymer period and can be made by optical lithography.

In all these examples, the removal of one block leaves a structure made from the other block, typically PS, that could be used as a mask for pattern transfer into a functional material. PS is, however, a rather poor mask, having a glass transition temperature of 100 °C and relatively low etch resistance. In addition, in these block copolymers, a small but significant number of defects (dislocations or disinclinations) remain, which is undesirable for nanolithographic applications. The defect population is related to the Flory–Huggins interaction parameter, χ , which describes the driving force for microphase separation in the block copolymer. Block copolymers with higher χ have a higher driving force for reducing the defect population, and are therefore more desirable for achieving long-range ordering.¹⁶

The ideal block copolymer for nanolithography applications therefore exhibits both a high value of χ and one highly etch-resistant block. Poly(styrene-*b*-dimethylsiloxane) (PS–

* Corresponding author. E-mail: caross@mit.edu.

PDMS) block copolymers satisfy both criteria. The high density of Si in the backbone of PDMS provides extremely high etch contrast between the two blocks when treated in an oxygen plasma, which is advantageous for pattern transfer into underlying materials, and the large interaction parameter χ enables the formation of ordered structures with a large correlation length. Moreover, PDMS has been widely utilized in soft lithography and micro/nanofluidic devices, and ordered PDMS block copolymer patterns may be expected to have extensive applications in nano- and biological technologies.¹⁷ PS–PDMS has been studied in the bulk¹⁸ and has been used in forming polymer blends,¹⁹ but its templating behavior and applications in nanolithography have not yet been reported. Here, we report the formation of defect-free robust nanoscale line patterns from PS–PDMS with an orientation that can be controlled by the annealing conditions and template geometry, and their use as etch masks for nanolithography.

A diblock copolymer of PS–PDMS with overall molecular weight of 45.5 kg/mol and volume fraction of PDMS $f_{\text{DMS}} = 33.5\%$ was custom-made by Polymer Source, Inc. The substrates used in this experiment consisted of smooth or trench-patterned Si substrates with native oxide layers. The 40 nm deep periodic trench patterns were fabricated using a Lloyd's Mirror interference lithography system with a 325 nm wavelength He–Cd laser²⁰ to expose grating patterns in a trilayer resist, combined with reactive ion etching to transfer the grating into the substrate. The period of the trenches was close to 1 μm , and the mesa width was varied between 125 and 500 nm. In some experiments, the surfaces were modified by hydroxy-terminated PS or PDMS homopolymer with molecular weight 5 kg/mol, which was spun-cast on the substrates and annealed at 150 °C for 15 h and then washed with toluene to remove unreacted material.¹⁴ The thickness of the grafted brush layer was estimated to be around 3–4 nm by ellipsometry.

Thin films 35 nm thick were obtained by spin-casting toluene solutions of 1.5% by weight of the block copolymer on the substrates, and then the samples were solvent-annealed under toluene vapor at room temperature for 4–70 h. The vapor pressure of toluene was controlled via the ratio R between the surface area of the liquid solvent and the volume of the annealing chamber. During solvent annealing, the block copolymer flows from the mesas to the trenches.⁹ The as-spun block copolymer film thickness was chosen so that, after solvent annealing, a monolayer of cylinders was present within the trenches while the mesas were left clear of cylinders. The annealed film was treated with a 5 s, 50 W CF_4 plasma then a 90 W O_2 plasma to remove the PS leaving oxygen-plasma-modified PDMS cylinders on the substrate. The surface morphology was observed using a Zeiss/Leo Gemini 982 scanning electron microscope (SEM) operated with an acceleration voltage of 5 kV. A thin layer of Au–Pd alloy was sputter-coated on the samples in order to avoid charging effects.

The surface tension of PDMS ($\gamma = 19.9 \text{ mN/m}$) is lower than that of PS ($\gamma = 40.7 \text{ mN/m}$),²¹ and thus PDMS preferentially segregates at the air/polymer interface.²² This

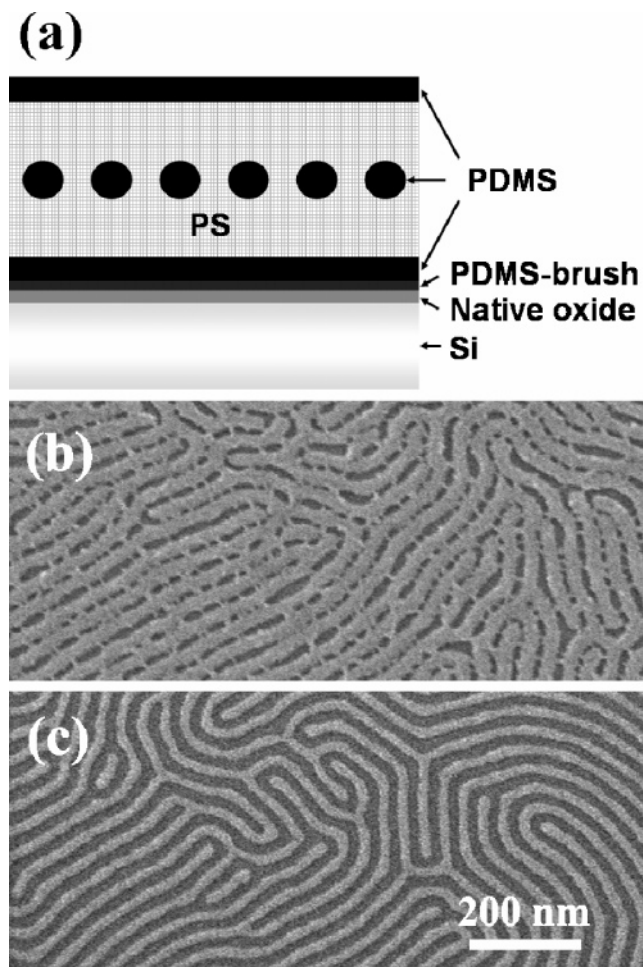


Figure 1. (a) Schematic cross-section diagram of a film of PS–PDMS on a PDMS brush-treated silica surface. A layer of PDMS is present at the air–film interface, and below it a layer of parallel cylinders. (b,c) SEM images of PS–PDMS thin film after (b) exposure to an O_2 plasma for 1 min; (c) exposure to a CF_4 plasma (5 s) followed by an O_2 plasma (1 min).

produces the structure shown schematically in Figure 1a for a film formed on a PDMS–brush coated substrate. The thin continuous PDMS surface layer is resistant to an oxygen plasma, and an oxygen etch alone fails to produce sharp domain patterns (Figure 1b). Therefore, a short (5 s) CF_4 plasma treatment was performed to remove the PDMS surface layer before the oxygen plasma processing. Figure 1c shows the results of this etching, which on a smooth substrate produces well-defined in-plane cylinder patterns without long-range order.

The maze structure in Figure 1c is characterized by low edge roughness. The edge roughness is believed to scale with the thickness of the intermaterial dividing surface (IMDS), which delineates the two blocks. The IMDS geometry is determined by the condition that interfacial energy is minimized and chain conformational entropy is maximized.²³ The χ parameter of PS–PDMS ($\chi \sim 0.26$)²⁴ at room temperature is considerably larger than those of PS–PMMA ($\chi \sim 0.06$),²⁵ poly(styrene-*b*-isoprene) ($\chi \sim 0.09$),²⁶ poly(styrene-*b*-2-vinylpyridine) ($\chi \sim 0.18$),²⁷ and poly(styrene-*b*-ethylene oxide) ($\chi \sim 0.08$),²⁸ leading to a thinner IMDS and low pattern edge roughness.

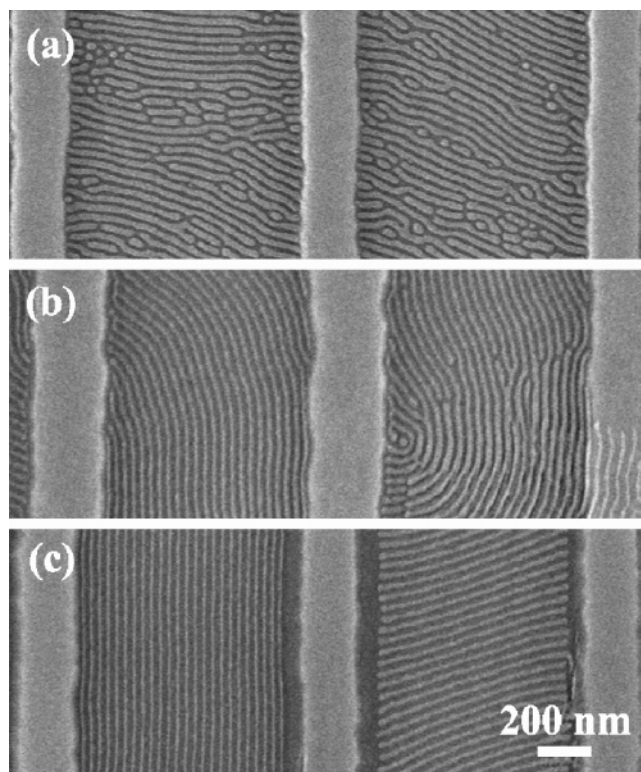


Figure 2. SEM images of PS–PDMS on trench substrates (a) without a brush, (b) with a PS–brush, and (c) with a PDMS brush. The samples were solvent-annealed for 15 h.

To illustrate the role of surface chemistry, parts a–c of Figure 2 shows the cylinder morphology on three different trench-patterned substrates precoated with no brush, a PS–brush, and a PDMS–brush, respectively. The PS–PDMS on bare Si (Figure 2a) shows a disordered structure with some perpendicular and some in-plane cylinders, which is assumed to result from the strong interaction between the PDMS block and the hydroxyl-terminated polar native oxide surface. Such interactions impede the diffusivity of the polymer on the surface, leading to nonequilibrium morphologies, as found for polybutadiene.²⁹ On a PS–brush coated substrate (Figure 2b), uniform cylinders form, but the ordering within the trenches is poor. In this case, island formation is observed (for example, at bottom right of the figure) because a smaller thickness of polymer is required to form one monolayer of cylinders on a brush composed of the majority component of the diblock copolymer.²⁹ On a PDMS–brush coated surface (Figure 3c), the degree of ordering of the cylinders within the trenches is markedly improved, and correlation lengths of tens of micrometers are observed in some trenches. This contradicts the proposal that a brush made of the minority block should have little effect on ordering of a block copolymer in which the minority block preferentially wets the substrate.²⁹ These remarkable differences are attributed to the extremely low surface energy of the PDMS surface. The flexibility of the Si–O backbone enables the molecules of the brush layer to adsorb on the silica surface presenting their methyl groups upward.³⁰ This provides a very low energy barrier for surface diffusion of the PS–PDMS diblock

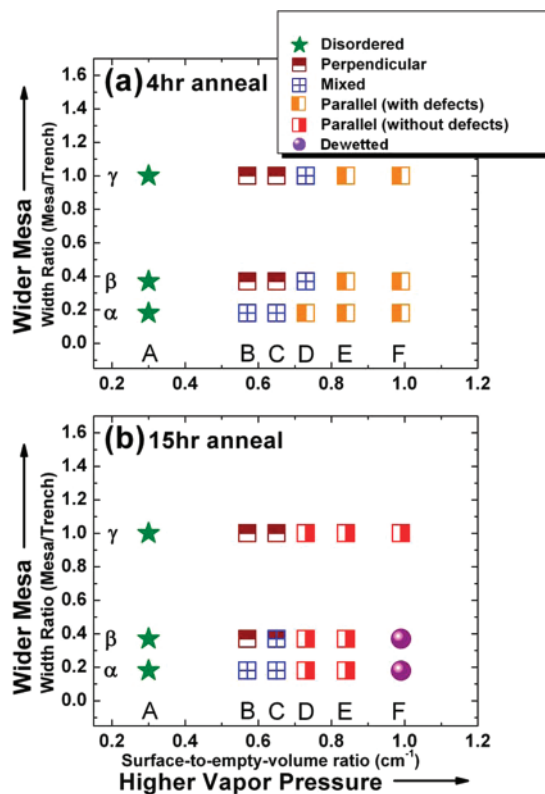


Figure 3. Arrangement of cylinders as a function of mesa/trench width ratio and solvent vapor pressure for (a) $t_{\text{anneal}} = 4$ h and (b) $t_{\text{anneal}} = 15$ h. For condition C β in (b), both perpendicular and mixed orientations were observed.

copolymer. These results suggest that a PDMS brush might be also effective for self-organization of other block copolymers.

We will now show how the collective effects of mesa width, solvent vapor pressure, and annealing time can be used to control the alignment of cylinders in trenches with a PDMS brush. In this experiment, the period of the topographic patterns was set to $1 \mu\text{m}$, and the width ratio of mesa to trench was varied from 0.18 to 1. The solvent vapor pressure was varied by changing the solvent surface area to annealing chamber volume ratio R within the range of 0.3 cm^{-1} (designated condition A) to 0.99 cm^{-1} (condition F). A higher vapor pressure causes the polymer to swell, lowers the glass transition temperature, and facilitates rearrangement of the polymer chains. The effect of R on swelling was evident from the color of the samples, which changed from gray (as-spun) to gold, violet, or blue for conditions A–F.

Parts a and b of Figure 3 show systematic trends in the cylinder morphology as a function of solvent vapor pressure R and trench geometry (mesa width/trench width at constant periodicity) for two different annealing times. A low solvent vapor pressure (condition A) gives only disordered cylinders regardless of the trench geometry. In contrast, under a high vapor pressure (condition F), the cylinders align parallel to the trench edges at an early stage of annealing (4 h, Figure 3a) but eventually dewet (15 h, Figure 3b), particularly for wide trenches (designated α and β). At intermediate vapor pressures, the cylinders can align either parallel or perpendicular to the trench edges, and defect levels decrease with

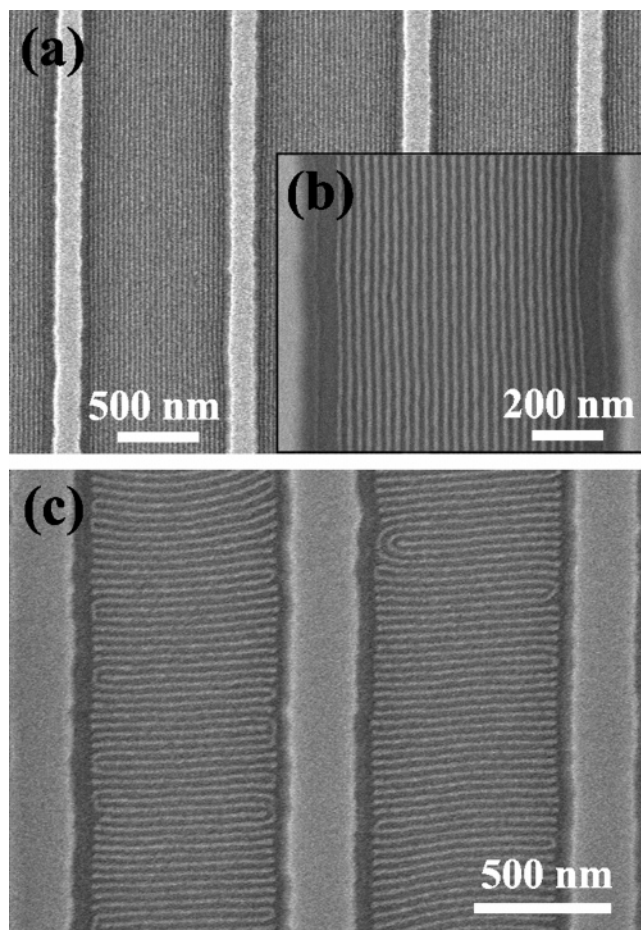


Figure 4. SEM images of (a,b) parallel cylinders on trench substrates with narrow mesas ($W_{\text{mesa}} = 125$ nm and $W_{\text{trench}} = 875$ nm) under a high vapor pressure of toluene (condition E α from Figure 3) and (c) perpendicular cylinders in a wide-mesa pattern ($W_{\text{mesa}} = 270$ nm and $W_{\text{trench}} = 730$ nm) at a lower vapor pressure (condition B β). The annealing time was 15 h.

increasing annealing time. At condition E, a parallel alignment of cylinders containing defects such as Y-junctions is observed after 4 h annealing, while 15 h annealing gives virtually defect-free patterns over a large scale substrate (1 cm²), as shown in Figure 4a,b, except near the edge of the sample, where the as-spun film thickness is higher. Cylinders with a width of 16 nm and a period of 34 nm were aligned in each trench. The number of cylinders in each trench depends on its width; for example, in Figure 4a, 26 cylinders are visible. This degree of ordering on a macroscopic scale is attributed to the large χ parameter of PS–PDMS and exceptionally low surface energy of the PDMS–brush grafted on the native oxide surface.

The ability to orient cylinders either perpendicular or parallel to the trenches by controlling the trench geometry and annealing conditions is of particular interest in nanolithography applications. Trenches with wide mesas (β and γ) and relatively low vapor pressure annealing (B and C) lead to uniformly or predominantly perpendicular orientation (Figure 4c), despite the higher free energy of the ends of the cylinders.³¹ Perpendicular alignment of cylinders in local areas of trenches has been reported and attributed to capillary flow from mesas to trenches, perpendicular to the trench

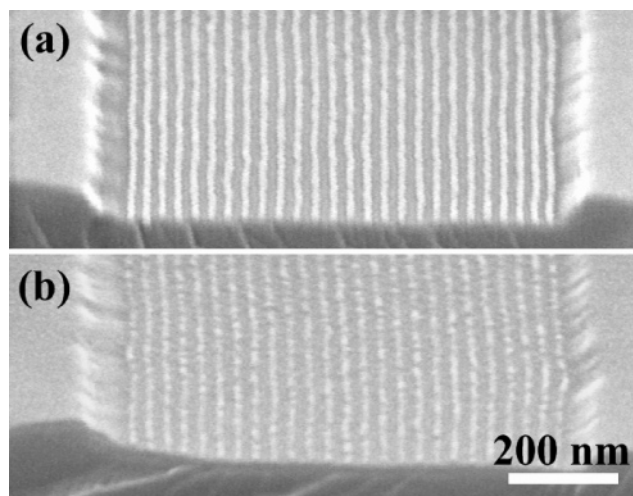


Figure 5. Tilted SEM images (a) before and (b) after CF₄ RIE for 30 s, in which the cylinder patterns were transferred into an underlying thin silica film; (a) shows 26 cylinders, while (b) from a different part of the sample, shows 25 silica “nanowires”.

walls.⁹ Such a flow will be greater for higher mesa/trench ratios, and this mechanism could account for the observation of perpendicular cylinders only for the higher width ratios β and γ . The perpendicular or mixed orientation is metastable and is gradually replaced by the parallel orientation (see conditions C β , D β , D γ) for longer annealing times.

To illustrate pattern transfer from the PDMS cylinders into an underlying 20 nm silica layer, a 300W CF₄ reactive ion etch was performed for 30 s. Cross section images before and after pattern transfer are presented in Figure 5a,b. The 20 nm silica was fully etched (the etch rate of silica under these conditions is 0.7 nm/s) to produce “wires” that are narrower than the width of the initial oxidized PDMS cylinders due to partly isotropic etching. An etched silica layer can be used as a mask for subsequent etching by reactive ion etching or ion milling⁶ or to form a large-area nanoimprint mold.

In summary, a PS–PDMS block copolymer has been investigated for applications in self-assembled nanolithography. This material combines the advantages of a high χ parameter, leading to well-ordered structures with low edge roughness and a high etch selectivity between the two blocks, providing etch-resistant masks for pattern transfer. A topographical PDMS–brush coated silica surface can be used to template in-plane cylinder arrays with long-range order. Moreover, the cylinder arrays may be selectively oriented parallel or perpendicular to the trench walls by control of solvent annealing and mesa width, and the pattern can be transferred into the underlying silica. These well-controlled nanoscale PDMS patterns may have a variety of applications in the fabrication of narrow interconnect lines, nanoimprint lithography stamps, or nanofluidic devices.

Acknowledgment. We gratefully acknowledge the support of the Semiconductor Research Corporation and a Korean Graduate Fellowship, and thank H. I. Smith and K. K. Berggren for the use of laboratory facilities.

References

- (1) Chou, S. Y.; Krauss, P. R.; Zhang, W.; Guo, L. J.; Zhuang, L. *J. Vac. Sci. Technol. B* **1997**, *15*, 2897.
- (2) Piner, R. D.; Zhu, J.; Xu, F.; Hong, S. H.; Mirkin, C. A. *Science* **1999**, *283*, 661.
- (3) Park, M.; Harrison, C.; Chaikin, P. M.; Register, R. A.; Adamson, D. H. *Science* **1997**, *276*, 1401.
- (4) Bates, F. S.; Fredrickson, G. H. *Annu. Rev. Phys. Chem.* **1990**, *41*, 525.
- (5) Vega, D. A.; Harrison, C. K.; Angelescu, D. E.; Trawick, M. L.; Huse, D. A.; Chaikin, P. M.; Register, R. A. *Phys. Rev. E* **2005**, *71*, 061803.
- (6) Cheng, J. Y.; Ross, C. A.; Chan, V. Z. H.; Thomas, E. L.; Lammertink, R. G. H.; Vancso, G. J. *Adv. Mater.* **2001**, *13*, 1174.
- (7) Thurn-Albrecht, T.; Schotter, J.; Kastle, C. A.; Emley, N.; Shibauchi, T.; Krusin-Elbaum, L.; Guarini, K.; Black, C. T.; Tuominen, M. T.; Russell, T. P. *Science* **2000**, *290*, 2126.
- (8) Kim, S. H.; Misner, M. J.; Russell, T. P. *Adv. Mater.* **2004**, *16*, 2119.
- (9) Sundrani, D.; Darling, S. B.; Sibener, S. J. *Langmuir* **2004**, *20*, 5091.
- (10) Sundrani, D.; Sibener, S. J. *Macromolecules* **2002**, *35*, 8531.
- (11) Black, C. T.; Bezencenet, O. *IEEE Trans. Nanotechnol.* **2004**, *3*, 412.
- (12) Black, C. T. *Appl. Phys. Lett.* **2005**, *87*, 163116.
- (13) Kim, S. O.; Solak, H. H.; Stoykovich, M. P.; Ferrier, N. J.; de Pablo, J. J.; Nealey, P. F. *Nature* **2003**, *424*, 411.
- (14) Stoykovich, M. P.; Muller, M.; Kim, S. O.; Solak, H. H.; Edwards, E. W.; de Pablo, J. J.; Nealey, P. F. *Science* **2005**, *308*, 1442.
- (15) Hawker, C. J.; Russell, T. P. *MRS Bull.* **2005**, *30*, 952–966.
- (16) Bang, J.; Kim, S. H.; Drockenmuller, E.; Misner, M. J.; Russell, T. P.; Hawker, C. J. *J. Am. Chem. Soc.* **2006**, *128*, 7622.
- (17) Unger, M. A.; Chou, H. P.; Thorsen, T.; Scherer, A.; Quake, S. R. *Science* **2000**, *288*, 113.
- (18) Chu, J. H.; Rangarajan, P.; Adams, J. L.; Register, R. A. *Polymer* **1995**, *36*, 1569.
- (19) Chuai, C. Z.; Li, S.; Almdal, K.; Alstrup, J.; Lyngaae-Jorgensen, J. *J. Appl. Polym. Sci.* **2004**, *92*, 2747.
- (20) Ross, C. A.; Haratani, S.; Castano, F. J.; Hao, Y.; Hwang, M.; Shima, M.; Cheng, J. Y.; Vogeli, B.; Farhoud, M.; Walsh, M.; Smith, H. I. *J. Appl. Phys.* **2002**, *91*, 6848.
- (21) Chan, C. M. *Polymer Surface Modification and Characterization*, 1st ed.; Hanser Publishers: Munich, 1994.
- (22) Andersen, T. H.; Tougaard, S.; Larsen, N. B.; Almdal, K.; Johannsen, I. *J. Electron Spectrosc. Relat. Phenom.* **2001**, *121*, 93.
- (23) Gido, S. P.; Schwark, D. W.; Thomas, E. L.; Goncalves, M. D. *Macromolecules* **1993**, *26*, 2636.
- (24) Nose, T. *Polymer* **1995**, *36*, 2243.
- (25) Bucholz, T. L.; Loo, Y. L. *Macromolecules* **2006**, *39*, 6075.
- (26) Ren, Y.; Lodge, T. P.; Hillmyer, M. A. *Macromolecules* **2000**, *33*, 866.
- (27) Hammond, M. R.; Cochran, E.; Fredrickson, G. H.; Kramer, E. J. *Macromolecules* **2005**, *38*, 6575.
- (28) Frielinghaus, H.; Hermsdorf, N.; Almdal, K.; Mortensen, K.; Messe, L.; Corvazier, L.; Fairclough, J. P. A.; Ryan, A. J.; Olmsted, P. D.; Hamley, I. W. *Europhys. Lett.* **2001**, *53*, 680.
- (29) Harrison, C.; Chaikin, P. M.; Huse, D. A.; Register, R. A.; Adamson, D. H.; Daniel, A.; Huang, E.; Mansky, P.; Russell, T. P.; Hawker, C. J.; Egolf, D. A.; Melnikov, I. V.; Bodenschatz, E. *Macromolecules* **2000**, *33*, 857.
- (30) Clarson, S. J.; Semlyen, J. A. *Siloxane Polymers*; PTR Prentice Hall: New York, 1993.
- (31) Cheng, J. Y.; Ross, C. A.; Smith, H. I.; Thomas, E. L. *Adv. Mater.* **2006**, *18*, 2505.

NL070924L